Supplementary Information for

Nickel doping as an effective strategy to promote the separation of photogenerated charge carriers for efficient solar-fuels production

Jin Wang[a], Yimin Xuan[a*], Kai Zhang[a]

[a.] School of Energy and Power Engineering, Nanjing University of Aeronautics and Astronautics, Nanjing, 210016, China

Email: ymxuan@nuaa.edu.cn

Experimental Section

Materials

Zinc nitrate ($Zn(NO_3)_2 \cdot 6H_2O$) was purchased from Kelong Chemical Reagent Co., Ltd (Chengdu, China), nickel nitrate ($Ni(NO_3)_2 \cdot 6H_2O$) was purchased from Aladdin and indium nitrate ($In(NO_3)_3 \cdot 5H_2O$), thioacetamide (CH_3CSNH_2, TAA), acetonitrile (CH_3CN), triethanolamine ($C_6H_{15}NO_3$, TEOA) were purchased from Macklin. All the chemicals were obtained from commercial sources of analytical reagent (AR) grade without further purification.

Synthesis of $ZnIn_2S_4$ and $ZnIn_2S_4$ -Ni

$ZnIn_2S_4$ nanosheets were synthesized through a hydrothermal method. In a typical procedure, 1mmol of $Zn(NO_3)_2 \cdot 6H_2O$, 2 mmol of $In(NO_3)_3 \cdot 5H_2O$ and 4 mmol of thioacetamide were dissolved in 50 mL ultrapure water under sonication, respectively. Then, the homogeneous solution was transferred into a 100 mL Teflon-lined autoclave and then heated at 180 °C for 18 h. After that, the mixture were allowed to cool to room temperature. The precipitates were collected by high-speed centrifugation, and washed with water and ethanol for several times. The final samples were dried in air at 80 °C for 12 h. To prepare Ni doped $ZnIn_2S_4$ nanosheets, a calculated amount of $Ni(NO_3)_2 \cdot 6H_2O$ was added into the above mixed solution under ultrasonic treatment before transferring into the autoclave. $ZnIn_2S_4$ doped with different amounts of Ni is denoted as ZIS-Ni-x; the value of x, from 0 wt% to 5 wt%, is used to describe the weight content of Ni relative to ZIS.

Characterizations

The X-ray diffraction (XRD) patterns of the samples were collected on a Bruker D8 Advance X-ray diffractometer with Ni-filtered Cu Kα radiation at 40 kV and 40 mA, with 2θ ranging from 10^o to 85^o and a scan rate of 0.02^o per second. Raman measurements were acquired at room temperature using a Raman Spectrometer (LabRAM HR Evolution, HORIBA) with a 325 nm emitting laser as an excitation source. The weight percentage of Ni was analyzed by Inductively

Coupled Plasma Optical Emission Spectrometer (ICP-OES, Agilent, 720). X-ray photoelectron spectroscopy (XPS) measurements were performed by a ESCALAB 250Xi spectrometer (Thermo Scientific, USA) using Al Kα radiation X-ray source (hν = 1486.6 eV) to determine the chemical states and the valence states of involved elements. The adventitious carbon C 1s peak located at 284.6 eV is used as the reference binding energy. The micromorphology was characterized by a field emission scanning electron microscope (SEM, Zeiss, GeminiSEM 300) and a field emission transmission electron microscope (TEM, Thermo scientific, FEI Talos F200S). The Brunauer-Emmett-Teller (BET) and N_2 sorption isotherms test was obtained from micromeritics ASAP 2460. The samples were degassed in vacuum at 100 °C for 4 h, and then measured at 78 K to determine N_2 sorption, respectively. The pore size distribution was calculated from the Barrett-Joyner-Halenda (BJH) method for micropore and mesoporous. The optical absorption properties were quantified by a UV-visible absorption spectrometer (Perkin Elmer, Lambda 1050) equipped with an integrating sphere. Steady-state PL spectra were measured using an Edinburgh Instruments, FLS 1000 equipped with a Xe lamp at room temperature under the excitation of 375 nm. Time-resolved PL decay curves were recorded on a FLS 1000 fluorescence lifetime spectrophotometer under the excitation of 375 nm and probed at 460 nm.

Photoelectrochemical measurements

The photoelectrochemical measurements were performed with an electrochemical workstation (Zahner Zennium, Germany) in a standard three electrode cell at room temperature. Platinum foil is used as the counter electrode, and a Ag/AgCl (saturated KCl) electrode is used as the reference electrode. The working photoanodes were fabricated as follows: 4 mg as-synthesized samples, 1 mL ethanol and 20 µL Nafion (Macklin) were mixed by sonication for 30 min to make a slurry. 0.5 mL solution is taken out and then dropped onto a fluorine-doped tin oxide (FTO) glass and dried at room

temperature. The active areas of the photoanodes are ≈ 1 cm^2. All the curves were measured in 0.5 M Na_2SO_4 aqueous solution, prior to all measurements, the electrolyte was purged with Ar for 30 minutes. The photoelectrochemical performance was mainly investigated by photocurrent-time (I-T) and electrochemical impedance spectroscopy (EIS). The photocurrent measurements were performed under simulated solar light irradiation by a 300W Xe lamp and EIS was carried out in the frequency range of 0.05 – 10^6 Hz. To study the surface reaction kinetics of as-synthesized samples, LSV test was conducted in the high gas tightness single chamber three electrode reactor (Figure S2, P60-45, Beijing Perfect Light Technology Co., Ltd.) with the same electrochemical workstation (Zahner Zennium, Germany) with photoelectrochemical measurements. The experiment was carried out under Ar and CO_2 atmosphere to investigate the surface reaction kinetics of both H_2 evolution and CO_2 reduction reaction. The reactor was filled with 84 mL 0.5 M Na_2SO_4 aqueous solution under Ar, and 42mL of acetonitrile, 28 mL of H_2O and 14 mL of TEOA under CO_2 to simulate the photocatalytic reaction solutions. Then the reactor interface was sealed with paraffin films to ensure the air-tightness. Ar gas was bubbled into the solutions for 1h to remove dissolved oxygen. CO_2 gas was bubbled for another 30 min before the CO_2 reduction reaction test to make sure CO_2 was saturated in the reaction solution. LSV curves were tested with a scan rate of 50 mV/s.

Photocatalytic Activity Test

Photocatalytic activity tests were carried out in a 50 mL Schlenk flask reactor with a silicone rubber septum (Figure S1). A 300 W Xe lamp (Microsolar 300, Beijing Perfect Light Technology Co., Ltd.) was used as light source with the electric current at 10 A. For photocatalytic hydrogen evolution, 10 mg photocatalyst, 10 mL of H_2O and 2 mL of TEOA were added into the reactor. For photocatalytic CO_2 reduction, 10 mg photocatalyst, 6 mL of acetonitrile, 4 mL of H_2O and 2 mL of TEOA were added into the reactor. The solution was

ultrasonicated for 30 min. Before starting the photocatalytic reaction, the solution was bubbled with Ar gas for 1h to remove dissolved oxygen. For photocatalytic CO_2 reduction, high purity CO_2 was then bubbled into the reactor for another 30 min with a partial pressure of 1 atm. The reaction system was vigorously stirred by a magnetic stirrer and irradiated under the 300 W Xe lamp with a wavelength range of 320 - 780 nm. The reaction system was kept at room temperature. The gases produced from the reaction were sampled using a vacuum tight syringe and analyzed using a GC9720 plus gas chromatography (GC, Zhejiang Fuli Analytical Instrument Co., Ltd China) equipped with a thermal conductivity detector (TCD) and a flame ionization detector (FID) every 6h. The CO is converted to CH_4 via a methanation reactor and CH_4 is detected by an FID. The $^{13}CO_2$ isotope labeling experiment was performed under the same photocatalytic reaction condition. The reactor containing 10 mg of the catalyst, 6 mL of acetonitrile, 4 mL of H_2O and 2 mL of TEOA was first was bubbled with Ar gas for 1h to ensure air removal and then filled with $^{13}CO_2$ gas (99 atomic% ^{13}C; Aldrich). After 10 hours of irradiation, 1 ml of gas products was sampled using a gas-tight syringe and then injected into a GC-MS (Agilent, GC Model 7890N/MS Model 5977B) for analysis.

Figure S1 The image of 50 mL Schlenk flask reactor.

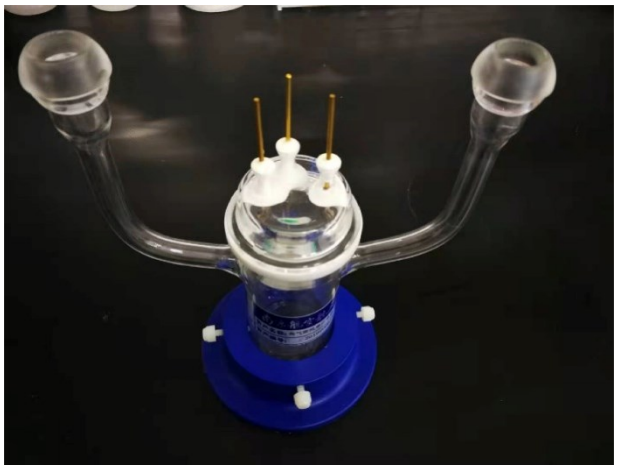

Figure S2 The image of high gas tightness single chamber three electrode reactor.

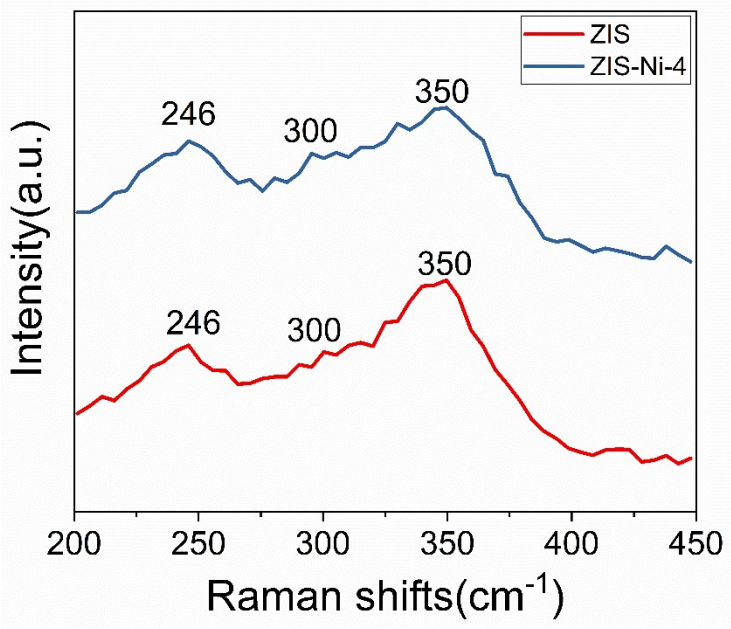

Figure S3 Raman spectra of ZIS and ZIS-Ni-4.

Raman spectrum was also used to investigate the structure of the as-synthesized samples. As depicted in Fig S3, three peaks around 246, 300, and 350 cm^{-1} are attributed to the longitudinal optical mode (LO_1), transverse optical mode (TO_2) and longitudinal optical mode (LO_2) mode of crystalline ZIS, respectively. No additional peaks can be detected in ZIS and ZIS-Ni-4, further excluding other crystalline impurity[1].

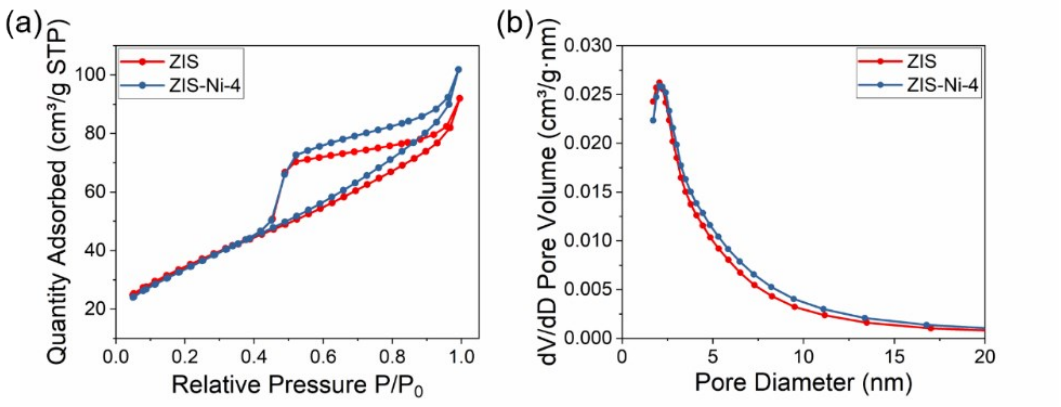

Fig. S4 (a) Nitrogen adsorption-desorption isotherms and (b) the corresponding pore size distribution curves of ZIS and ZIS-Ni-4.

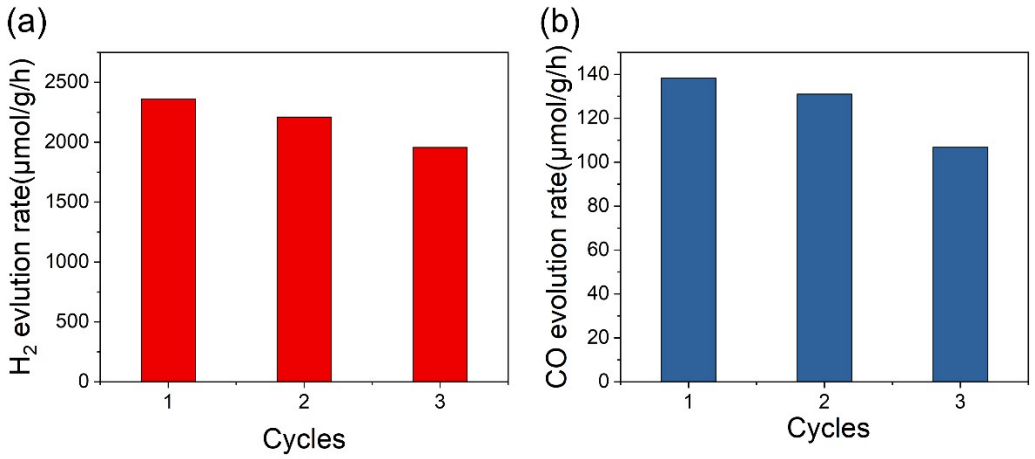

Fig.S5 Recycled (a) H_2 evolution and (b) CO reduction performance of ZIS and ZIS-Ni-4.

The cycling experiments were performed to study the photocatalytic stability of ZIS-Ni-4. Apparently, the photocatalytic performance of ZIS-Ni-4 for H_2 evolution and CO reduction remains basically unchanged during three cycles. The yield of H_2 and CO only decreases slightly after three cycles of 18 h, which may because of the catalyst loss during the experiment process.

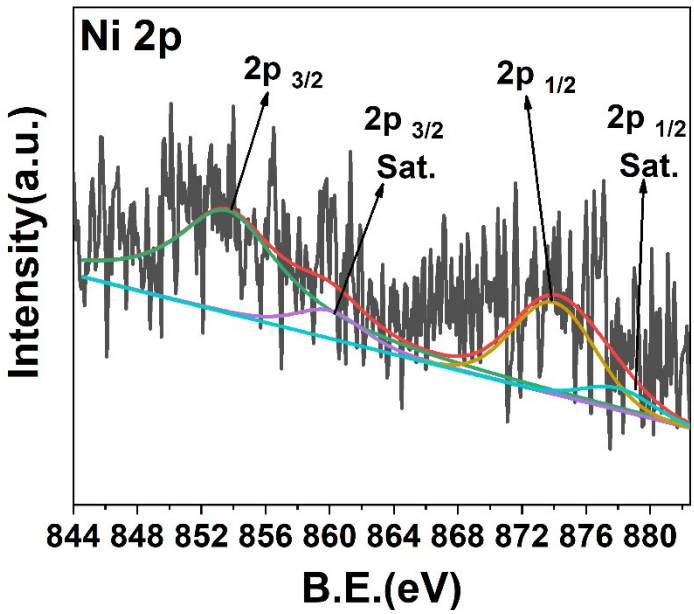

Fig S6 The XPS spectra of Ni in the as synthesized ZIS-Ni-4 after the photocatalytic reaction

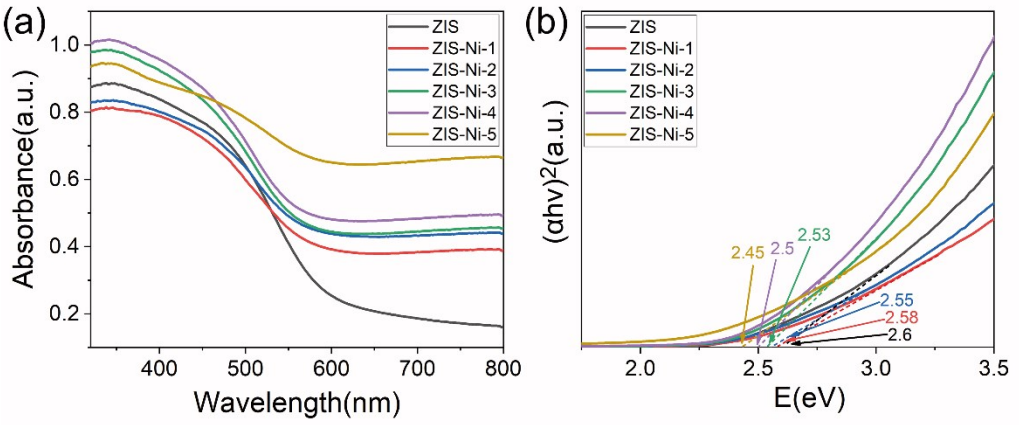

Fig. S7 (a) UV–vis diffuse reflectance spectra of ZIS and ZIS-Ni-x. (b) Tauc plots together with the band gap of ZIS and ZIS-Ni-x.

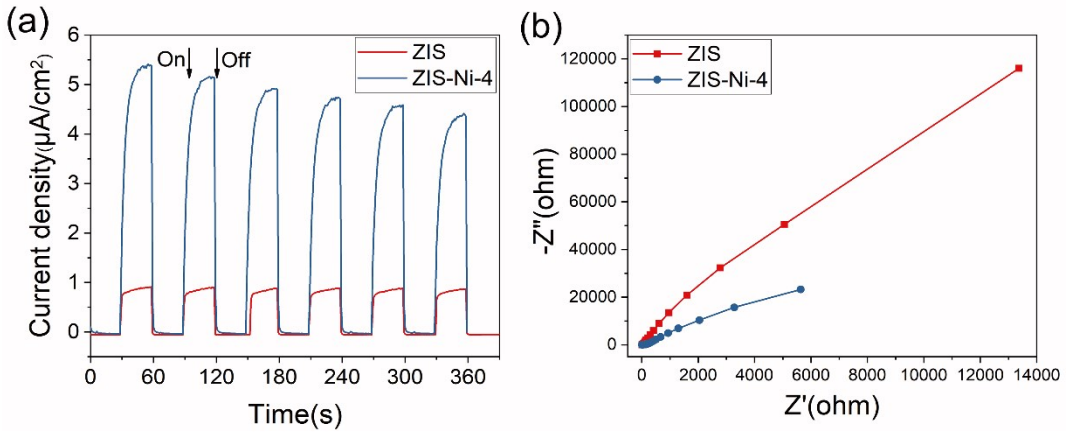

Fig.S8 (a) The transient photocurrent responses and (b) Nyquist plots of ZIS and ZIS-Ni-4.

To further study the role of Ni doping in enhancing the photocatalytic activity, photoelectrochemical (PEC) measurements, including transient photocurrent responses and electrochemical impedance spectroscopy (EIS) are measured to investigate the photogenerated charge transfer behavior of the as-synthesized samples. As depicted in Fig S8a, the transient photocurrent intensity of ZIS-Ni-4 is remarkably enhanced compared to pure ZIS, indicating that doped Ni can promote a more efficient separation and migration of photogenerated charge carriers. Furthermore, electrochemical impedance spectra (EIS) was carried out under dark conditions. The Nyquist plots of pure ZIS and ZIS-Ni-4 are shown in Fig S8b, the diameter of the semicircle arc for ZIS-Ni-4 is much smaller than that of ZIS, suggesting

its lower interfacial charge-transfer resistance and thus indicating that doped Ni can also accelerate the interfacial photogenerated charge transfer.

Table S1 The Ni contents of ZIS and ZIS-Ni-4 measured by ICP-OES and theoretical calculation

Sample	Ni (wt%) ICP-OES	Ni (wt%) theoretical
ZIS	0	0
ZIS-Ni-4	4.40	4

Table S2 XPS Peak Table of ZIS-Ni-4

Elements	Atomic (%)	Calculated mass ratio (%)
Zn	13.24	17.9
In	24.23	57.4
S	34.19	22.6
Ni	1.73	2.1

Table S3 The BET surface area and pore parameters of ZIS and ZIS-Ni-4

Sample	BET Surface Area (m^2/g)	BJH Adsorption volume of pores (cm^3/g)	BJH Desorption volume of pores(cm^3/g)	BJH dsorption average pore diameter (nm)	BJH Desorption average pore diameter (nm)
ZIS	124.7	0.12	0.13	4.3	3.8
ZIS-Ni-4	124.9	0.15	0.16	5.2	4.5

Table S4 A comparison with other photocatalysts in CO2 reduction

Catalyst	Irradiation source (Xe lamp)	Products	Evolution rate (μmol/g/h)	Reference
ZnIn2S4-Ni	300 W	H2	H2: 1479.3	This work

		CO	CO: 138.3	
ZnS:Ni/[Ru(dpbpy)]	500 W	CO	CO: 1.72	2
		HCOOH	HCOOH: 6.25	
3D(V_{Zn})- ZnIn2S4	300 W	CO	276.7	3
One-Unit-Cell ZnIn2S4	300 W	CO	33.2	4
CuGaS2/CdS	300 W	H2	H2: 17	5
		CO	CO: 0.75	
Nitrogen-rich g-C_3N_4 nanotubes	300 W	CO	103.6	6
O/La-g-C_3N_4	300 W	CO	92	7

1. X. Shi, L. Mao, C. Dai, P. Yang, J. Zhang, F. Dong, L. Zheng, M. Fujitsuka and H. Zheng, *Journal of Materials Chemistry A*, 2020, **8**, 13376-13384.
2. T. M. Suzuki, T. Takayama, S. Sato, A. Iwase, A. Kudo and T. Morikawa, *Applied Catalysis B: Environmental*, 2018, **224**, 572-578.
3. Y. He, H. Rao, K. Song, J. Li, Y. Yu, Y. Lou, C. Li, Y. Han, Z. Shi and S. Feng, *Advanced Functional Materials*, 2019, **29**, 1905153.
4. X. Jiao, Z. Chen, X. Li, Y. Sun, S. Gao, W. Yan, C. Wang, Q. Zhang, Y. Lin, Y. Luo and Y. Xie, *Journal of the American Chemical Society*, 2017, **139**, 7586-7594.
5. S. Wu, H. Pang, W. Zhou, B. Yang, X. Meng, X. Qiu, G. Chen, L. Zhang, S. Wang, X. Liu, R. Ma, J. Ye and N. Zhang, *Nanoscale*, 2020, **12**, 8693-8700.
6. Z. Mo, X. Zhu, Z. Jiang, Y. Song, D. Liu, H. Li, X. Yang, Y. She, Y. Lei, S. Yuan, H. Li, L. Song, Q. Yan and H. Xu, *Applied Catalysis B: Environmental*, 2019, **256**, 117854.
7. P. Chen, B. Lei, X. a. Dong, H. Wang, J. Sheng, W. Cui, J. Li, Y. Sun, Z. Wang and F. Dong, *ACS Nano*, 2020, **14**, 15841-15852.